Veterinary Immunology and Immunopathology 216 (2019) 109919

Contents lists available at ScienceDirect

Veterinary Immunology and Immunopathology

journal homepage: www.elsevier.com/locate/vetimm

Research paper

WC1^{+} and WC1^{neg} γδ T lymphocytes in intestinal mucosa of healthy and *Mycobacterium avium* subspecies *paratuberculosis*-infected calves

Latasha Ludwig, Rebecca Egan, Monica Baquero, Amanda Mansz, Brandon L. Plattner*

Department of Pathobiology, Ontario Veterinary College, University of Guelph, Guelph, Ontario, N1G 2W1, Canada

ARTICLE INFO

Keywords:
Bovine
Immunology
gamma delta T cells
Mucosal immunity
Mycobacterium avium subspecies *paratuberculosis*

ABSTRACT

Mucosal surfaces such as the gastrointestinal tract, and skin are the front line of host defence and immunity against many pathogens. Gamma delta (γδ) T lymphocytes preferentially localize to the mucosal surfaces in several species including cattle, and are thought to play crucial roles in immunosurveillance and host defence, particularly against mycobacteria. Many γδ T cells are present in young calves, which is the period when calves are thought to be initially exposed to *Mycobacterium avium* subspecies *paratuberculosis* (*Map*). The role of mucosal γδ T cells in cattle, especially during host-pathogen interactions during early pre-clinical phases of infectious disease remains unclear. The purposes of this study were to investigate and characterize WC1^{+} and WC1^{neg} γδ T cell subsets in various segments of the gastrointestinal (GI) tract of young calves, and then to examine γδ T cell subsets in the distal small intestine of calves after experimental intestinal *Map* infection by direct Peyer's patch inoculation. We show that in healthy calves, the relative proportion of γδ T cells is constant throughout the GI mucosa, though the ileum has significantly more γδ T cells. In the distal intestine, γδ T cells are mainly WC1^{neg} and primarily located within the lamina propria of the jejunum and ileum. In *Map*-infected intestine, there are higher numbers of γδ T cells in the lamina propria and a greater proportion of WC1^{+} cells within the epithelial layer compared to control calves. While WC1^{neg} γδ T cells preferentially localize to the distal small intestine of healthy calves, WC1^{+} γδ T cells are increased in the intestinal mucosa during *Map* infection, which is suggestive of effector cell function. Further, spectral microscopy and flow cytometry in tandem will lead to improved understanding of the functions of these cells during health and disease.

1. Introduction

Mucosal surfaces are the interface of the body with the external environment, and as such are the front lines of host defence and immunity against many pathogens. It is here where either success or failure of the initial host defence mechanisms are thought to permit establishment or mediate clearance of infectious agents (Ewer et al., 2006). Gamma delta (γδ) T lymphocytes have been studied in humans, mice, and cattle, and they are known to play several roles during innate and adaptive immune responses, particularly against intracellular pathogens (Plattner and Hostetter, 2011). Because γδ T cells preferentially localize to mucosal surfaces, it is thought that they play an important role in immunosurveillance and/or defence against agents and potential pathogens (Wyatt et al., 1994; Plattner and Hostetter, 2011). γδ T lymphocytes only represent 1–5% of circulating lymphocytes in humans and mice (Komori et al., 2006), but up to 50% of intraepithelial T cells in mice (Fujihashi et al., 1994). Cattle have a higher proportion of γδ T cells in peripheral blood compared to most species, especially the young, where up to 40–50% of all CD3^{+} blood lymphocytes express the γδ T cell receptor (Davis et al., 1996; Wyatt et al., 1994; Baquero and Plattner, 2017a). The percentage of γδ T cells in peripheral blood declines with age (Baquero and Plattner, 2017a), but it is unknown if the same is true for intestinal γδ T cells (Wyatt et al., 1994; Coussens, 2001). Importantly, studying peripheral blood-derived cells may not reflect the function of γδ T cells at the tissue level in health or disease.

Ruminants have two major distinct subpopulations of γδ T cells based on the presence or absence of the workshop cluster (WC) 1 molecule (Herzig and Baldwin, 2009). WC1 is a γδ T cell specific scavenger receptor cysteine-rich glycoprotein that is thought to function as an activating co-receptor and/or pattern recognition surface molecule. WC1^{+} and WC1^{neg} subpopulations exhibit tissue-specific tropism (Machugh et al., 1997; Yasuda et al., 2005), and WC1 variants define pathogen responsiveness and probably overall function of these cells (Telfer and Baldwin, 2015; Damani-Yokota et al., 2018). WC1^{+} γδ T cells localize predominantly to the peripheral blood, spleen, skin and intestinal lamina propria (Machugh et al., 1997); they are readily

* Corresponding author.
E-mail address: bplattne@uoguelph.ca (B.L. Plattner).

https://doi.org/10.1016/j.vetimm.2019.109919
Received 13 March 2019; Received in revised form 22 July 2019; Accepted 5 August 2019

accessed *via*the peripheral blood compartment, and as such these are the most widely studied subset in cattle. In contrast, tissue distribution and mechanisms of $WC1^{neg}$ γδ T cells, which are rare in blood and preferentially localize to mucosal surfaces and spleen, are understudied and remain poorly understood (Machugh et al., 1997; Johnson et al., 2008). We have observed that $WC1^{+}$ and $WC1^{neg}$ γδ T cells alter the effector function of autologous co-cultured macrophages and dendritic cells during *in vitro Mycobacterium avium* subspecies *paratuberculosis* (*Map*) infection of calves (Baquero and Plattner, 2017a, 2017b). Previous *in vitro* studies showed that bovine γδ T cells are recruited to mycobacterial infection sites and generate pro-inflammatory and regulatory cytokines that may influence the development of localized immune responses (Chiodini and Davis, 1992; Plattner et al., 2009; Rusk et al., 2017), but additional work characterizing the function of γδ T cells in tissues is necessary.

The intracellular bacterium *Map* is the causative agent of Johne's disease in ruminants, a disease that results in significant economic losses in the North American cattle industry annually (Coussens, 2001; McKenna et al., 2006). *Map* exposure usually occurs in young animals by ingestion of contaminated colostrum or milk (Sweeney, 1996). *Map* crosses the mucosal barrier through M cells overlying Peyer's patches of the distal ileum, is phagocytized by macrophages in the lamina propria, and establishes persistent infection for an extended subclinical phase prior to progression to clinical disease (Momotani et al., 1988). However, not all *Map*-exposed calves progress to clinical disease, and host-pathogen interactions at the site of intestinal *Map* infection may be critical in determining the success or failure of mycobacteria to persist locally in tissues (Russell, 2006). The outcome of mycobacterial infections is influenced by local immune responses including γδ T cells at initial infection sites (Plattner et al., 2009), and this may be key to understanding host resistance to infection (Verrall et al., 2013). Unfortunately, the pre-clinical stages of intestinal *Map* infection are exceedingly difficult and costly to study. A primary reason for this is that detection of *Map* in naturally infected animals is difficult due to poorly sensitive diagnostic tests; however, several experimental models allow investigation of various specific knowledge gaps regarding the immunopathology of *Map* infection (Hines et al., 2007; Begg et al., 2010; Plattner et al., 2011; Allen et al., 2009; Chandrashekhar et al., 2013; Mortier et al., 2013).

The purposes of this study were to characterize the presence of $WC1^{+}$ and $WC1^{neg}$ γδ T cell subsets in various segments of the gastrointestinal (GI) tract of healthy young bovine calves, and then to examine these γδ T cell subsets in the distal small intestine of calves following experimental intestinal *Map* infection by direct Peyer's patch inoculation (Plattner et al., 2011; Stinson et al., 2018). The overall hypotheses for this work were that $WC1^{+}$ and $WC1^{neg}$ bovine γδ T cell subsets are differentially distributed throughout the GI tract of bovine calves, and that these cells are recruited into the intestine during experimental localized *Map* infection. We also isolated γδ T cells directly from uninfected control and *Map*-infected calf intestine to compare the cell phenotype by flow cytometry with our microscopy data, which could be a beneficial technique for future functional analysis.

2. Materials and methods

2.1. Unexposed calves, tissue collection

In the first part of this study, we set out to describe the distribution of γδ T cell subsets at mucosal surfaces of the GI tract and skin in healthy six-month-old intact male Holstein calves with no *Map* exposure [n = 2]. All calves were sourced from the University of Guelph dairy teaching herd housed in Elora, Ontario. There is no Johne's disease herd certification program in Ontario; however, this herd is assumed free of Johne's disease based on repeated negative herd milk and individual cow serum antibody tests, and no clinical cases have been diagnosed in the herd for several years. For all live animals used in this study, their care and collection of tissue was performed following review and approval of AUP #1390 by the University of Guelph Animal Care Committee. Calves were euthanized at six months of age and the following tissue sections were collected and flash frozen in OCT compound in liquid nitrogen: skin, oropharynx, esophagus, abomasum, mid-jejunum, ileum, and colon. Sections of small intestine used in this study were subjected to *Map*-specific PCR as previously described (Stinson et al., 2018) to verify their *Map*-negative status.

2.2. Experimental Map-infection model, tissue collection

For the second part of this study, *Map*-inoculation of intact male Holstein calves was carried out at 30 days of age, by surgical inoculation with 10^9 colony-forming units of live *Map* strain gc86 in 0.5 mL sterile saline *via*direct injection in the Peyer's patch dense region of the distal ileum as previously described (Plattner et al., 2011; Stinson et al., 2018). *Map* exposed and unexposed control calves were housed in a biosafety-level II animal research facility on the main campus of the University of Guelph in groups of 2 and separately from each other to avoid cross-contamination of *Map*. Calves were euthanized 7 months post-*Map* exposure (8 months of age) [n = 2], along with age-matched unexposed controls [n = 2], and complete post-mortem examinations were performed. Sections of ileum 5 cm oral to the ileocecal valve at the level of the location of the *Map* inoculation site were collected and flash frozen in OCT medium. All sections of small intestinal tissue from these calves were subjected to *Map*-specific PCR as previously described (Stinson et al., 2018) to confirm the presence or absence of *Map* in these tissues. For this study, tissue sections for the *Map* positive group were selected only from *Map*-exposed calves who were then shown to be *Map* positive by PCR in the selected section, while tissue sections for the *Map* negative group were selected only from calves who were not *Map*-exposed and were then shown to be *Map* negative by PCR in all tissue sections.

2.3. Immunofluorescence and flow cytometry, antibodies

The following primary antibodies were used for immunofluorescence microscopy and flow cytometry: polyclonal rabbit anti-human CD3 (A0452, IgG, Dako Canada, Mississauga ON Canada), monoclonal mouse anti-bovine δ T cell receptor (TCR) (GB21A, IgG2b, Monoclonal Antibody Center (MAC), Washington State University (WSU), Pullman WA USA), and mouse anti-bovine WC1 (ILA29 (immunohistochemistry); BAQ4A (flow cytometry), IgG1, WSU). Primary antibodies were diluted in 2% bovine serum albumin (BSA) at the following concentrations for microscopy and flow cytometry, respectively: 1:1000 and 1:200 for CD3, 1:10,000 and 1:200 for δTCR, and 1:500 and 1:200 for WC1. The following secondary antibodies were used: Alexa Fluor (AF) 555-conjugated goat anti-mouse IgG2b paired with δTCR, AF647-conjugated goat anti-mouse IgG1 paired with WC1, and AF594 or AF488-conjugated goat anti-rabbit IgG paired with CD3 for microscopy or flow cytometry, respectively (all from Thermo Fisher Scientific Inc., Mississauga ON Canada). Secondary antibodies were diluted in 2% BSA at a concentration of 1:1000 for microscopy and 1:200 for flow cytometry.

2.4. Immunofluorescence labelling

Frozen tissue blocks for immunofluorescence labelling were sectioned at 6 microns using a Leica CM3050 S Cryostat and immediately fixed in 100% ethanol for 15 min at room temperature. Tissue sections were blocked for 30 min at room temperature with 10% normal goat serum (Cedarlane Canada, Burlington ON Canada) prior to application of the primary antibody cocktail of CD3, δTCR, and WC1, and incubated overnight in the dark at 4 °C. Slides were washed with phosphate buffered saline (0.01 M PBS, pH 7.3) prior to application of the secondary antibody cocktail of AF594 IgG, AF555 IgG2b, and AF647 IgG1 and

then incubated for 45 min in the dark at room temperature. Slides were then washed with PBS, and 4′,6′-diamidino-2-phenylindole (DAPI) nucleic acid stain (ThermoFisher Scientific, 1:30,000 in PBS) was applied for 1 min at room temperature. Slides were gently rinsed with PBS and a cover slip was then applied with anti-fade mounting media (4% n-propyl gallate (Sigma Aldrich, St. Louis MO USA) in 90% glycerol in 10% PBS). Controls followed the same general procedure as above and included individual primary and secondary antibody combinations (single colour controls), secondary antibodies cocktail only (negative controls, primary omitted), and tissue sections lacking both primary and secondary antibodies (negative controls, tissue auto-fluorescence correction).

2.5. Immunofluorescence microscopy

Images were captured using a multispectral imaging system (Quorum Technologies, Guelph ON Canada) which consists of the Nuance CRi multispectral camera mounted on an inverted Leica DMI 6000 brightfield widefield microscope. The mCherry cube (excitation wavelength: 542–582 nm; emission wavelength: 603–678 nm; wavelength range: 542–678 nm) with the TRITC filter (610 longpass (LP)) (for CD3, δTCR, and WC1) and DAPI cube (excitation wavelength: 352–402 nm; emission wavelength: 417–477 nm; wavelength range: 382–477 nm) with DAPI filter (420 L P) (for DAPI) were used to capture images as per manufacturer recommendation and wavelength profile. Multiple wavelengths were chosen using the mCherry cube with the TRITC filter from tissue sections pre-treated with normal goat serum and DAPI counter stain only (negative control) to establish a profile of tissue auto-fluorescence in each tissue type. Slides of each tissue section treated with 10% normal goat serum and secondary antibody cocktail were also examined to verify the absence of nonspecific binding by the secondary antibodies and no positive signal was detected (data not shown). Tissue sections of intestine labelled with single primary/secondary antibody combinations (CD3 with AF594, δTCR with AF555, and WC1 with AF647) were used to acquire individual fluorescent spectral signals with the mCherry cube and TRITC filter. For each tissue, three representative fields of view were captured with the 20X objective under the mCherry cube with TRITC filter, as well as the DAPI cube with DAPI filter, with the exception of the small intestinal sections, which were captured with the 40X objective due to the significantly greater numbers of fluorescently labelled cells present. Based on Metamorph calibrations of the Nuance CRi multispectral imaging system, 20X objective images were defined as a total image area of 353450.68 µm (0.4941 µm/pixel); 40X objective images were defined as a total image area of 88867.73 µm (0.2478 µm/pixel). As described by others (Mansfield et al., 2008), autofluorescence was removed using the earlier defined autofluorescence spectra, and images were unmixed using the Nuance Multispectral Imaging System software (CRi, PerkinElmer Canada) to acquire individual fluorescent signal images (AF594, AF555, AF647, DAPI). Some views required two images at different depths of tissue to enhance the focus of the image, and these images were combined as a Z-stack and the best focus derived image was used for analysis.

2.6. Image analysis

Merged composite images were created using Metamorph image analysis software (Molecular Devices Corp., California USA). The Z-stack images were visually thresholded (including background subtraction) to ensure that non-specific labelling (for example, out of plane of tissue section) was removed, while retaining cell-specific signal. Spectrally unmixed images of each individual fluorescent markers of interest (*i.e.*$CD3^+$, δTCR^+, or $WC1^+$) were individually merged with DAPI-stained images for cell quantification. Dual marker of interest composite merged images with DAPI were also created to confirm labelling patterns of each of the cell surface markers (*i.e.*to verify visually that δTCR^+ cells were also $CD3^+$, that $WC1^+$ cells were also δTCR^+, and that cell surface signals were appropriately associated with DAPI-positive nuclei). For the purpose of this study $CD3^+$ cells express AF594/CD3; γδ TCR^+ cells express both AF594/CD3 and AF555/δTCR; $WC1^+$ cells express AF647/WC1, AF555/δTCR and AF594/CD3; $WC1^{neg}$ cells express AF555/δTCR and AF594/CD3 markers but not AF647/WC1. Cell quantification was performed by a manual count of single marker positive cells. When fluorescent labelling in an image was uncertain, combined multiple fluorescent marker positive cell composite merged images were used ($CD3^+$/δTCR^+, δTCR^+/$WC1^+$). Total counts were collected for each cell type per field of view, and the following cell proportions were calculated: the percentage of γδ TCR^+ cells of the total number of $CD3^+$ cells, the percentage of $WC1^{neg}$ cells of the total number of γδ TCR^+ cells, and the percentage of $WC1^+$ cells of the total number of γδ TCR^+ cells. We also assessed the specific location of cells within either the epithelium or the lamina propria of the intestinal mucosa. A total of six fields were analyzed for each tissue (3 fields from each calf), and the average of these six fields was used to calculate total cell counts and proportions. The 40X objective images for γδ TCR^+ cell counts in the unexposed tissues were normalized to 20X objective images to facilitate comparison with these unexposed tissues in Fig. 1b by multiplying by the conversion factor 3.98 (20X area/40X area–per Nuance CRi multispectral camera set values).

2.7. Intestinal intraepithelial lymphocyte isolation

Five mm pieces of small intestine with Peyer's patches removed were transported to the laboratory on ice suspended in 40 mL of incubation buffer (Ca^{2+}- and Mg^{2+}- free HBSS supplemented with 2% FBS and 10% HEPES bicarbonate buffer). Intestinal pieces were washed

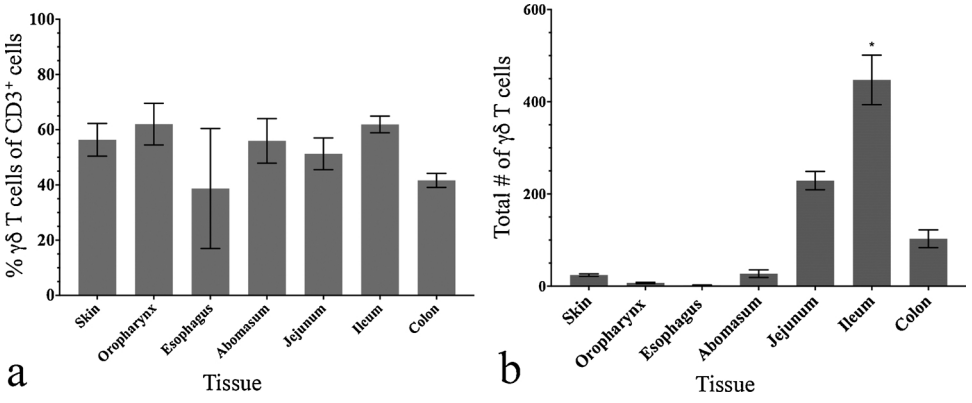

Fig. 1. Mucosal δTCR^+ cells in unexposed healthy six-month-old calves. (a) 39–62% of $CD3^+$ cells are δTCR^+; (b) Significantly more δTCR^+ cells are present in ileum compared to other mucosal surfaces (*$p \leq 0.0208$).

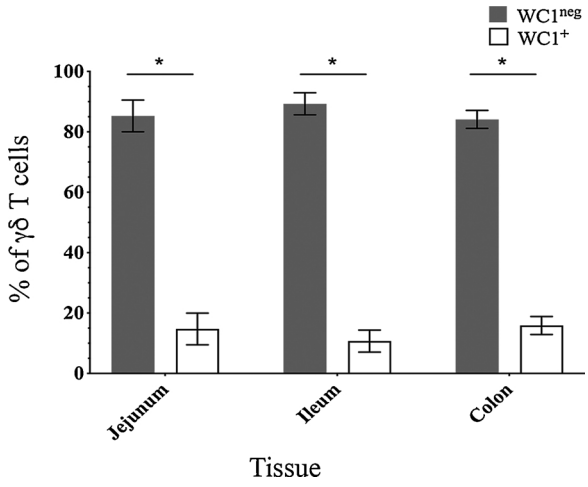

Fig. 2. WC1^{+} and WC1^{neg} δTCR^{+} cells in the small and large intestine of unexposed healthy six-month-old calves. The vast majority of γδ T cells in the distal intestine are WC1^{neg} (*p < 0.0001).

thoroughly with incubation buffer before incubating twice at 37 °C with stirring in incubation buffer with 10% FBS and 154 μg/mL of dithioerythritol (Sigma Aldrich). Intestinal pieces were then vortexed and passed through a 70 μm cell strainer and the resultant cell suspension containing intraepithelial lymphocytes and some epithelial cells was centrifuged at 400 x g for 5 min at 4 °C and the pellet was resuspended in 24 mL of 44% Percoll in RPMI 1640 (ThermoFisher Scientific). 8 mL of cell suspension was carefully layered over 5 mL of 67% Percoll in RPMI 1640. The tube was centrifuged at 600 × *g*for 20 min at room temperature. Intraepithelial lymphocytes were collected from the 44% to 67% interface, counted using a Moxi Z cell counter (Orflo Technologies, Ketchum Idaho USA) and stored at −80 °C in cryopreservation media (50% RPMI 1640 containing 2 mM of L-glutamine and 25 mM of HEPES supplemented with 5 × 10-5 M 2-mercaptoethanol with penicillin (1000 U/mL), streptomycin sulfate (10 mg/mL) and amphotericin B (0.25 μg/mL), 40% FBS, and 10% DMSO until further analysis.

2.8. Intestinal lamina propria lymphocyte isolation

After isolation of intestinal intraepithelial lymphocytes, intestinal pieces (collected during straining) were placed in a flask and stirred three times during one hour at 200 rpm at 37 °C with complete RPMI containing 100 U/mL of type VIII collagenase (Sigma Aldrich) and strained between digestions. The contents of the flask were then transferred into gentleMACS C tubes (Miltenyi Biotec, Bergisch Gladbach, Germany) and dissociated using the program m_brain_01 of the gentleMACS™ Dissociator (Miltenyi). The resultant cell suspension was centrifuged at 850 × *g*for 10 min. at 4 °C and supernatant was discarded. Cells were counted using a Moxi Z cell counter and stored at −80 °C in cryopreservation media for further analysis.

2.9. Flow cytometry, gating strategy

Cell viability was assessed using Zombie NIR fixable viability kit according to kit instructions (Biolegend CA USA). Cells were stained using the previously listed primary and secondary antibodies at their respective concentrations and per standard staining protocols. Briefly, primary antibodies (anti-human CD3, anti-bovine δ TCR and anti-bovine WC1) were applied as a cocktail to cell suspensions for 20 min at 4 °C. Cells were then washed thoroughly before secondary antibodies (AF488 paired with CD3; AF555 paired with δTCR; AF647 paired with WC1) were applied for 20 min at 4 °C. Cells were washed prior to proceeding to FACS, where data were acquired using FACS Aria IIu (BD Biosciences, Mississauga ON Canada) equipped with acquisition software FACS Diva II, and analyzed using FlowJo software (Treestar Inc., San Carlos CA USA). The lymphocyte region of interest was electronically gated based on side scatter (SSC) and forward scatter (FSC) properties, then non-viable cells were excluded. γδ TCR^{+} and WC1^{+} cell populations were sequentially identified from within the CD3^{+} cell population using electronic gates.

2.10. Statistical analysis

Statistical analysis of immunofluorescence microscopy and flow cytometry data was performed using SAS University (SAS Institute Inc., North Carolina USA). Mean values +/- standard error of mean (SEM) were calculated and a student *t*-test or one-way analysis of variances (ANOVA) was used to determine statistically significant differences, which was confirmed with a p value < 0.05 for each test.

3. Results

3.1. Distribution of γδ T cells in healthy calves

Approximately 50% [range 39–62%] of CD3^{+} T cells at mucosal surfaces and skin, were γδ TCR^{+} (Fig. 1a). No significant difference was observed in the proportion of γδ T cells at any of the mucosal sites examined in this study; however, the total number of γδ T cells varied significantly at different mucosal sites (Fig. 1b). The γδ TCR^{+} cells were predominantly observed in the small and large intestine, and rare γδ TCR^{+} cells were observed in the skin, oropharynx, esophagus and abomasum (Fig. 1b). Significantly more γδ TCR^{+} cells were present in the ileum compared with all other tissues examined (Fig. 1b, *p ≤ 0.0208). Because the γδ TCR^{+} cells were concentrated within the small and large intestine compared to all other sites examined, we went on to further characterize the phenotype of γδ TCR^{+} cells at these sites. In all three of these tissues, (jejunum, ileum, and colon), there were significantly more WC1^{neg} γδ T cells compared with WC1^{+} cells (80–85% compared with 15–20%, respectively, Fig. 2, *p < 0.0001).

We compared the spatial distribution of γδ TCR^{+} cells within the epithelium (intraepithelial lymphocytes) and the lamina propria of the small and large intestine. In the small intestine, a significantly higher percentage of γδ TCR^{+} cells were located within the lamina propria compared with the epithelium (Fig. 3; 60–65% *vs 35*–40% respectively, *p ≤ 0.0268). Most γδ TCR^{+} cells were located specifically within the superficial lamina propria of the small intestine adjacent to the

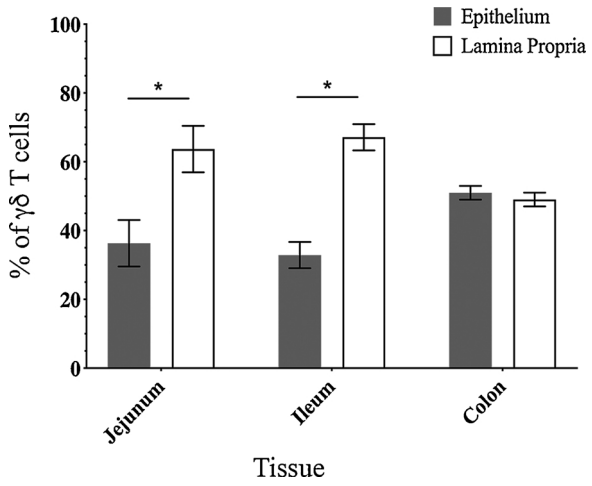

Fig. 3. Epithelium and lamina propria δTCR^{+} cells in the small and large intestine of unexposed healthy six-month-old calves. Most δTCR^{+} cells are in the lamina propria of small intestine (*p ≤ 0.0268), but are evenly distributed in colon.

epithelium-lamina propria interface, while CD3$^+$ γδ TCR^{neg} cells were randomly distributed within both the epithelium and lamina propria. In contrast, colonic γδ TCR$^+$ cells were evenly distributed between the lamina propria and epithelium (Fig. 3). WC1$^+$ γδ TCR$^+$ cells were rarely observed within the epithelium.

3.2. Distribution of γδ T cells in Map-infected calves

Based on these data showing the highest number of γδ TCR$^+$ cells in the ileum of healthy, unexposed calves (which was the site of experimental *Map* exposure in our model, and also hypothesized to be the initial site of *Map* invasion in natural infection), we then examined how the distribution of γδ TCR$^+$ cells in the intestine of calves is altered after experimental intestinal *Map* infection. Seven months after direct experimental surgical intestinal *Map* inoculation, we collected distal ileal tissue and confirmed the presence of *Map* in these samples using a custom *Map*-specific PCR assay described by Stinson et al. (2018). All segments of ileum used for this portion of the study were first confirmed *Map*-positive or *Map*-negative by PCR for *Map*-infected calves or unexposed control calves, respectively. The total number of γδ TCR$^+$ cells in the ileal lamina propria of *Map*-infected calves was significantly higher compared to uninfected control calves (Fig. 4a, *p = 0.0100; Fig. 5). We also assessed the distribution of WC1$^+$ and WC1^{neg} γδ T cell subsets within the ileal mucosa of *Map*-infected and uninfected control calves, and found that regardless of intestinal *Map* infection status, 70–98% of γδ TCR$^+$ cells in both the epithelium and lamina propria were WC1^{neg} (Fig. 4b, *p < 0.0001; Fig. 5). Although more γδ TCR$^+$ cells were present in the lamina propria of *Map*-infected calves (Fig. 4a), the ratio of WC1$^+$ γδ TCR$^+$ to WC1^{neg} γδ TCR$^+$ cell populations in the lamina propria did not significantly differ in *Map*-infected calves compared to uninfected control calves (Fig. 4b); WC1$^+$ and WC1^{neg} γδ TCR$^+$ cells increase proportionally. We also observed a significantly higher percentage of WC1$^+$ γδ TCR$^+$ cells (and conversely, significantly lower percentage of WC1^{neg} γδ TCR$^+$ cells) in the ileal epithelium of *Map*-infected calves compared to uninfected control calves (Fig. 4b, **p = 0.0116).

3.3. Phenotype of intraepithelial and lamina propria-derived γδ T cells

We then used flow cytometry to examine γδ T cells isolated directly from the ileal epithelium or lamina propria of *Map*-infected and unexposed control calves to compare with our immunofluorescence microscopy data. Similar to the microscopy data, we observed a significantly higher percentage of γδ T cells isolated directly from the lamina propria of *Map*-infected calves compared to uninfected control calves (Fig. 6a, *p = 0.0198). The vast majority of γδ TCR$^+$ cells isolated from the epithelium and lamina propria of all calves were WC1^{neg} (Fig. 6b, *p < 0.012), which is also consistent with our microscopy data (Fig. 4b). The ratios of WC1$^+$ and WC1^{neg} γδ TCR$^+$ cells in the lamina propria were similar in *Map*-infected calves compared with uninfected control calves (Fig. 6b). Also corresponding to our microscopy data, we observed a significantly increased percentage of WC1$^+$ γδ TCR$^+$ cells (and a statistically significant decrease in the percentage of WC1^{neg} γδ TCR$^+$ cells) in the epithelium of *Map*-infected calves compared to uninfected control calves (Fig. 6b, **p = 0.0398).

4. Discussion

In this study, approximately 40–60% of CD3$^+$ cells at mucosal surfaces of healthy calves were γδ TCR$^+$. These data are similar to what is reported in mice, and parallels what is seen in the peripheral blood of young calves (Fujihashi et al., 1994; Wyatt et al., 1994; Davis et al., 1996; Baquero and Plattner, 2017a). The proportion of γδ T cells did not vary significantly between mucosal surfaces examined in this study; however, the jejunum, ileum, and colon had significantly more γδ T cells compared to other locations, which suggests these cells play an important role in the local host defences and immune responses in these tissues. The distal intestinal tract contains Peyer's patches, which are important immunologic sites and are likely where initial *Map* uptake occurs in the intestinal lumen of calves (Lugton, 1999). Preferential localization of γδ T cells to this anatomic location supports a role in surveillance or as early immune responders to infection. γδ T cells in the jejunum and ileum were primarily located in the superficial lamina propria along the epithelial interface, which also supports the hypothesis that γδ T cells function in antigen sampling. It has been suggested that the oropharyngeal tonsils play an important role in *Map* uptake after oral inoculation (Payne and Rankin, 1961; Waters et al., 2003), and in this study we observed low numbers of CD3$^+$ and γδ T cells in the oropharyngeal tonsils of healthy calves.

As previously discussed, γδ T cells have specific WC1 subsets that preferentially localize to different tissues, including the intestinal tract (Machugh et al., 1997; Yasuda et al., 2005). All segments of the intestine examined in this study contained significantly more WC1^{neg} compared with WC1$^+$ γδ TCR$^+$ cells. This is in contrast to skin in our study (data not shown) and data published by others showing more WC1$^+$ cells compared with WC1^{neg} cells (Machugh et al., 1997; Yasuda et al., 2005). This is also in contrast to the peripheral blood compartment in ruminants, where WC1$^+$ cells represent up to 60% of the population of

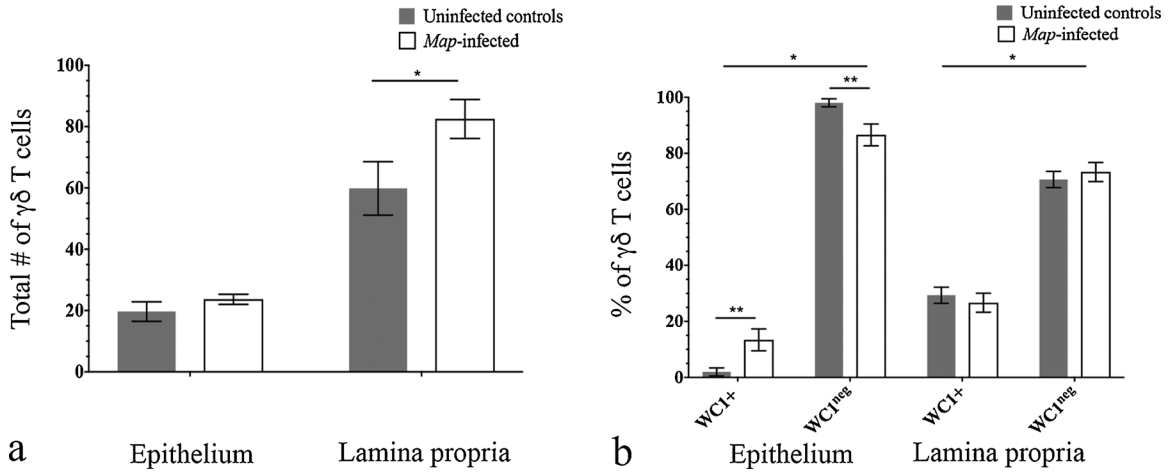

Fig. 4. Distribution δTCR$^+$ cells in ileum of *Map*-infected and control calves. (a) *Map*-infected calves had more δTCR$^+$ cells in the lamina propria compared to controls (*p = 0.0100). (b) Most intestinal δTCR$^+$ cells were WC1^{neg} (*p < 0.0001); *Map*-infected calves had significantly higher percentage of WC1$^+$ cells in the epithelium compared with controls (**p = 0.0116).

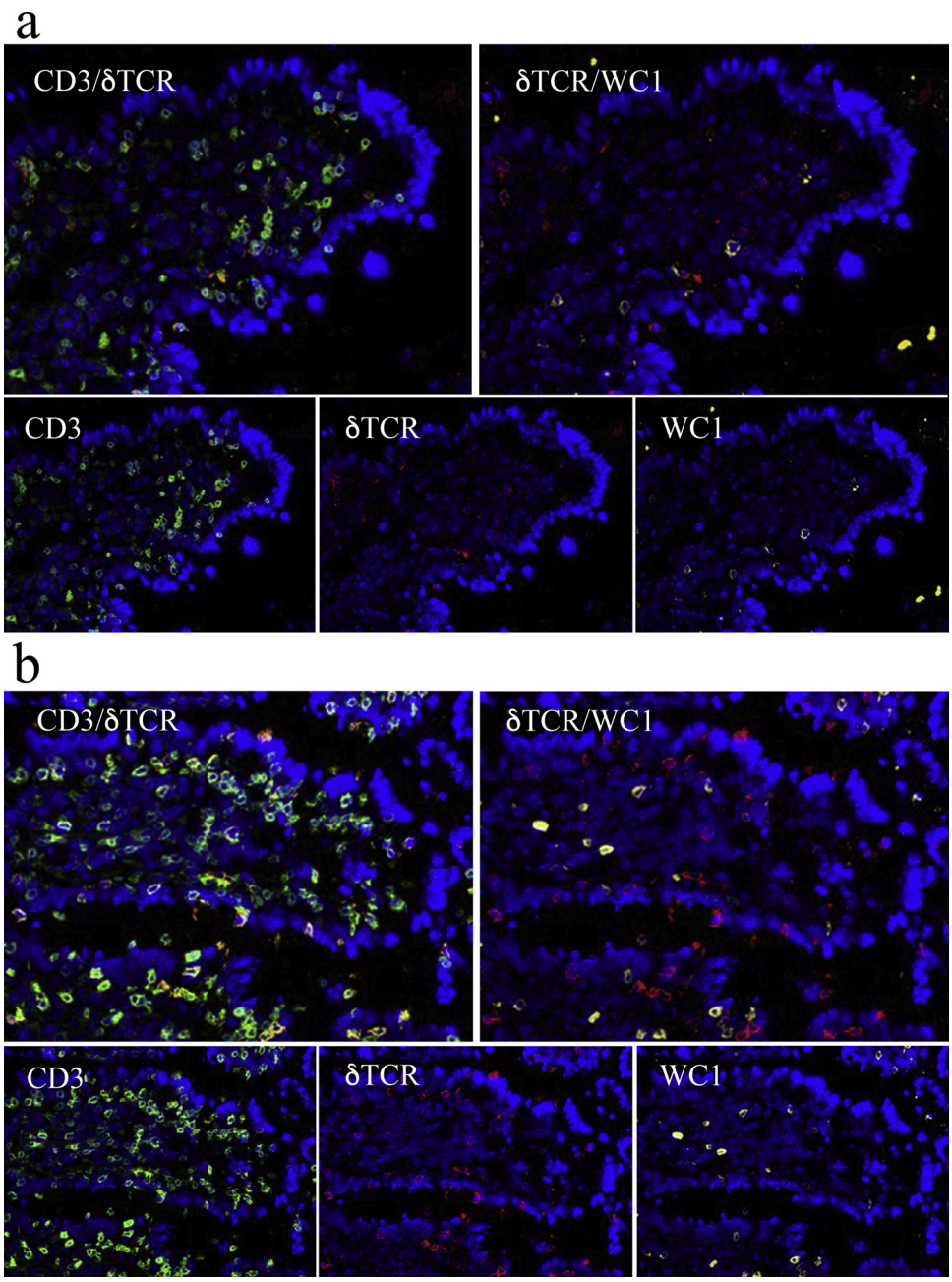

Fig. 5. T cell subsets in ileum of control (a) and *Map*-infected (b) calves, immunofluorescence microscopy, frozen section (40X objective images). $CD3^{+}\delta TCR^{+}$ cells are preferentially located in superficial lamina propria in all calves (a, b). *Map*-infected calves have significantly more $CD3^{+}\delta TCR^{+}$ cells (b) compared with control (a) calves. Most δTCR^{+} cells are $WC1^{neg}$ in all calves (a, b). There are significantly more $WC1^{+}$ δTCR^{+} cells in the epithelium of *Map*-infected (b) compared to control (a) calves. Overlay images of $CD3^{+}$/ δTCR^{+} (top left) and $WC1^{+}$ δTCR^{+} (top right) are shown in both panels along with single colour markers; $CD3^{+}$ (green), δTCR^{+} (red) and $WC1^{+}$ (yellow).

γδ T cells (Park et al., 2000) whereas in the small and large intestine, $WC1^{+}$ cells represent only 10–15% of $\gamma\delta TCR^{+}$ cells (Fig. 2). The $WC1^{neg}$ population comprises a low percentage in peripheral blood at only 3–5% of all blood γδ T cells (Park et al., 2000), but represents up to 90% of γδ T cells in the intestine. Data show that $WC1^{neg}$ cells respond to mycobacterial infections in calves, and they appear in highest numbers within days of *Map*-induced lesions of naïve calves (Plattner et al., 2009). Because they are preferentially located within the epithelial layer of mucosal surfaces of healthy calves as we observed in this study, it is likely that $WC1^{neg}$ γδ T cells serve a primary immunosurveillance role at mucosal surface of calves (Plattner et al., 2011). $WC1^{+}$ cells are also considered early immune effector cells, and are recruited to *Map*-induced lesions following previous antigenic priming, including vaccination or previous infection (Plattner et al., 2009; Machugh et al., 1997). Defining specific γδ T cell subpopulations along with their sites of localization and primary functions—especially at mucosal surfaces—is critical to understanding host defences and local immune responses to *Map* and other pathogens (Coussens, 2001).

The ileum is of particular interest because it contains significantly more γδ T cells than other mucosal tissues examined in this study, and it is the site of host-pathogen interactions during early infection and preclinical disease due to *Map* infection (Clarke, 1997; Begara-McGorum et al., 1998). Here we observed significantly more γδ T cells in the lamina propria of *Map*-infected calves by both microscopy and flow cytometry. Previous data have shown that peripheral blood γδ T cells proliferate during mycobacterial exposure in humans or following vaccination in calves; however, it is unknown if this occurs in tissues of cattle or other species (Häcker et al., 1992; de Silva et al., 2005).

During *Mycobacterium bovis* infection in calves, peripheral blood $WC1^{+}$ cells decrease and it is hypothesized that this is due to migration to infection sites (Pollock and Welsh, 2002). This is important because tissue distribution may differ significantly from blood (Pollock and Welsh, 2002), and studying only peripheral blood does not facilitate a full understanding of cellular responses. The intestinal mucosa has not been extensively studied, but our findings suggest that migration of $WC1^{+}$ γδ TCR^{+} cells from peripheral blood into the mucosa of the

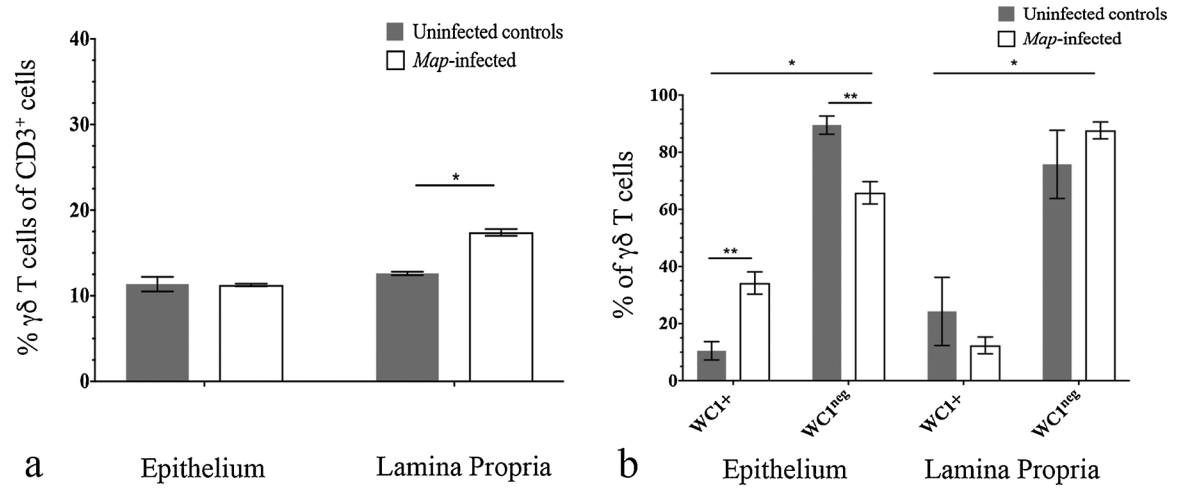

Fig. 6. Distribution δTCR$^+$ cells in ileum of *Map*-infected and control calves by flow cytometry. (a) Significantly higher proportion of δTCR$^+$CD3$^+$ cells are present in lamina propria of *Map*-infected compared to control calves (*p = 0.0198). (b) Most δTCR$^+$ cells in small intestine are WC1^{neg} (*p < 0.012), but *Map*-infected calves have significantly more WC1$^+$ δTCR$^+$ cells in the epithelium (**p = 0.0398).

intestine occurs in response to *Map* infection. This is based on our observation of increased WC1$^+$ cells within the intestine after direct intestinal *Map* inoculation, though WC1^{neg} cells remain the predominant subset in the intestine after *Map* infection. This further supports the hypothesis that WC1^{neg} γδ TCR$^+$ cells are uniquely positioned along the superficial gastrointestinal mucosa for host defence, but that both WC1^{neg} and WC1$^+$ cells are important in host pathogen interactions during intestinal *Map* infection in calves.

We used spectral microscopy and flow cytometry as complementary techniques for examination of γδ T cell distribution and phenotype *in situ* and *ex vivo*. Spectral microscopy provides a unique opportunity to focus on specific regions of interest during *Map* infection in the intestine of calves, and this allows identification of spatial arrangements not accessible by quantitative methods alone. Flow cytometry provides an objective measurement to not only validate our microscopy data, but also to sample a greater volume/weight of tissue, and to determine if subsets of intestinal γδ TCR$^+$ cells could be sufficiently collected for future functional studies. Using these methods together will allow us to gain a better understanding of cell function and distribution while investigating their responses to pathogens.

In this study, we acknowledge that characterization of T cell subsets in a small number of animals at a single time point does not allow us to fully understand a complex and evolving disease process such as enteric *Map* infection; however, the differences are interesting and establish rationale for future work focusing on γδ T cell distribution and subpopulations at several time points in a larger cohort of animals. Importantly, this small sample also allowed us to test the agreement between spectral microscopy and flow cytometric analyses with an eye to future functional studies. Because spectral microscopy allows examination of distinct regions giving unique perspective into various disease processes, future sites of interest to better understand this disease are the ileal dome regions which are thought to be specific site of *Map* entry into the host. Finally, determining the expression of cytokines by specific subsets of intestinal cells will help to further define their role in the initial immune response and defence of the host. Further investigation will build a more complete understanding of host-pathogen interactions in the intestine, and may provide crucial insight into key aspects of the host immune response that lead either to the control and clearance of *Map*, or to the establishment of persistent intestinal infection, and would have significant impact on Johne's disease control in the cattle industry.

Funding

This work was supported by the National Sciences and Engineering Research Council of Canada (NSERC) Discovery grant (#400715 to BLP) and by the Ontario Veterinary College personal research funds (#071882 to BLP). All calf work was also supported by the Ontario Ministry of Agriculture and Rural Affairs grant (#200479 to BLP).

Acknowledgements

The exceptional animal care technicians at the University of Guelph Animal housing facility have been previously acknowledged; however, this project would not have been possible without their support. For assistance in collection of tissues, Mili Kulkarni is also gratefully acknowledged.

References

Allen, A.J., Park, K.T., Barrington, G.M., Lahmers, K.K., Hamilton, M.J., Davis, W.C., 2009. Development of a bovine illeal cannulation model to study the immune response and mechanisms of pathogenesis of paratuberculosis. Clin. Vaccine Immunol. 16 (4), 453–463.

Baquero, M.M., Plattner, B.L., 2017a. Bovine peripheral blood WC1 + and WC1neg gd T lymphocytes modulate monocyte-derived macrophage effector functions during *in vitro Mycobacterium avium* subspecies *paratuberculosis* infection. Cell. Immunol. 315, 34–44.

Baquero, M.M., Plattner, B.L., 2017b. Bovine WC1 + and WC1neg gd T lymphocytes influence monocyte differentiation and monocyte-derived dendritic cell maturation during *in vitro Mycobacterium avium* subspecies *paratuberculosis* infection. Front. Immunol. 8 (534), 1–11.

Begara-McGorum, I., Wildblood, L.A., Clarke, C.J., Connor, K.M., Stevenson, K., Mcinnes, C.J., Sharp, J.M., Jones, D.G., 1998. Early immunopathological events in experimental ovine paratuberculosis. Vet. Immunol. Immunopathol. 63, 265–287.

Begg, D.J., de Silva, K., Di Fiore, L., Taylor, D.L., Bower, K., Zhong, L., Kawaji, S., Emery, D., Whittington, R.J., 2010. Experimental infection model for Johne's disease using a lyophilised, pure culture, seedstock of *Mycobacterium avium* subspecies *paratuberculosis*. Vet. Microbiol. 141, 301–311.

Chandrashekhar, C., Gonzalez-Cano, P., Fries, P., Gomis, S., Doig, K., Scruten, E., Potter, A., Napper, S., Griebel, P.J., 2013. Host responses to persistent *Mycobacterium avium* subspecies *paratuberculosis* infection in surgically isolated bovine ileal segment. Clin. Vaccine Immunol. 20 (2), 156–165.

Chiodini, R.J., Davis, W.C., 1992. The cellular immunology of bovine paratuberculosis: the predominant response is medicated by cytotoxic gamma/delta T lymphocytes which prevent CD4+ activity. Microb. Pathogen. 13 (6), 447–463.

Clarke, C.J., 1997. The pathology and pathogenesis of paratuberculosis in ruminants and other species. J. Comp. Pathol. 116, 217–261.

Coussens, P.M., 2001. *Mycobacterium paratuberculosis* and the bovine immune system. Anim. Health Res. Rev. 2 (2), 141–161.

Damani-Yokota, P., Telfer, J.C., Baldwin, C.L., 2018. Varigated transcription of the WC1 hybrid PRR/co-receptor genes by individual gamma delta T cells and correlation with pathogen responsiveness. Front. Immunol. 9 (717), 1–12.

Davis, W.C., Brown, W.C., Hamilton, M.J., Wyatt, C.R., Orden, J.A., Khalid, A.M.,

Naessens, J., 1996. Analysis of monoclonal antibodies specific for the gamma-delta TcR. Vet. Immunol. Immunopathol. 52, 275–283.
De Silva, K., Plain, K.M., Begg, D.J., Purdie, A.C., Whittington, R.J., 2005. CD4 + T cells, gamma-delta T cells and B cells are associated with lack of vaccine protection in *Mycobacterium avium* subspecies *paratuberculosis* infection. Vaccine 33 (1), 149–155.
Ewer, K., Millington, K.A., Deeks, J.J., Alvarez, L., Bryant, G., Lalvani, A., 2006. Dynamic antigen-specific T-cell response exposure to Mycobacterium tuberculosis. Am. J. Respir. Crit. Care Med. 174 (7), 831–839.
Fujihashi, K., Yamamoto, M., McGhee, J.R., Kiyono, H., 1994. Function of alpha-beta TCR + and gammadelta TCR + IELs for the gastrointestinal immune response. Int. Rev. Immunol. 11, 1–14.
Häcker, G., Kromer, S., Heeg, K., Ivanyi, J., Wagner, H., Pfeffer, K., 1992. Opportunist mycobacteria express ligands that stimulate production of human Vy9V82 T lymphocytes. Infect. Immun. 60 (7), 2753–2757.
Herzig, C.T., Baldwin, C.L., 2009. Genomic organization and classification of the bovine WC1 genes and expression by peripheral blood gamma delta T cells. BMC Genomics 10 (1), 1.
Hines II, M.E., Stabel, J.R., Sweeney, R.W., Griffin, F., Thalaat, A.M., Bakker, D., Benedictus, G., Davis, W.C., de Lisle, G.W., Gardner, I.A., Juste, R.A., Kapur, V., Koets, A., McNair, J., Pruitt, G., Whitlock, R.H., 2007. Experimental challenge models for Johne's disease: a review and proposed international guidelines. Vet. Microbiol. 122, 197–222.
Johnson, W.C., Bastos, R.G., Davis, W.C., Goff, W.L., 2008. Bovine WC1- gdT cells incubated with IL-15 express the natural cytotoxicity receptor CD335 (NKp46) and produce IFN-g in response to exogenous IL-12 and IL-18. Dev. Comp. Immunol. 32 (8), 1002–1010.
Komori, H.K., Meehan, T.F., Havran, W.L., 2006. Epithelial and mucosal gamma delta T cells. Curr. Opin. Immunol. 18, 534–538.
Lugton, I., 1999. Mucosa-associated lymphoid tissues as sites for uptake, carriage and excretion of tubercle bacilli and other pathogenic mycobacteria. Immunol. Cell. Biol. 77, 364–372.
Machugh, N.D., Mburu, J.K., Coral, M.J., Wyatt, C.R., Orden, J.A., Davis, W.C., 1997. Identification of two distinct subsets of boving gd T cells with unique cell surface phenotype and tissue distribution. Immunol. 92, 340–345.
Mansfield R., J., Hoyt, C., Levenson M., R., 2008. Visualization of Microscopy-Based Spectral Imaging Data from Multi-Label Tissue Sections. Current Protocols in Molecular Biology 84 (1), 1–15.
McKenna, S.L.B., Keefe, G.P., Tiwari, A., VanLeeuwen, J., Barkema, H.W., 2006. Johne's disease in Canada Part II: disease impacts, risk factors, and control programs for dairy producers. Can. Vet. J. 47 (11), 1089–1099.
Momotani, E., Whipple, D.L., Thiermann, A.B., Cheville, N.F., 1988. Role of M cells and macrophages in the entrance of Mycobacterium paratuberculosis into domes of ileal Peyer's patches in calves. Vet. Pathol. 25 (2), 131–137.
Mortier, R.A.R., Barkema, H.W., Bystrom, J.M., Illanes, O., Orsel, K., Wolf, R., 2013. Evaluation of age-dependent susceptibility in calves infected with two doses of *Mycobacterium avium* subspecies *paratuberculosis* using pathology and tissue culture. Vet. Res. 44 (1), 94.
Park, Y.H., Yoo, H.S., Yoon, J.W., Yang, S.J., An, J.S., Davis, W.C., 2000. Phenotypic and functional analysis of bovine gd lymphocytes. J. Vet. Sci. 1 (1), 39–48.
Payne, J.M., Rankin, J.D., 1961. The pathogenesis of experimental Johne's disease in calves. Res. Vet. Sci. 2, 167–174.
Plattner, B.L., Chiang, Y.W., Roth, J.A., Platt, R., Hu man, E., Zylstra, J., Hostetter, J.M., 2011. Direct inoculation of *Mycobacterium avium* subspecies *paratuberculosis* into ileocecal Peyer's patches results in colonization of the intestine in a calf model. Vet. Pathol. 48, 584–592.
Plattner, B.L., Doyle, R.T., Hostetter, J.M., 2009. Gamma-delta T cell subsets are differentially associated with granuloma development and organization in a bovine model of mycobacterial disease. Hip Int. 90 (6), 587–597.
Plattner, B.L., Hostetter, J.M., 2011. Comparative gamma delta T cell immunology: a focus on mycobacterial disease in cattle. Vet. Med. Int. 2011, 1–8.
Pollock, J.M., Welsh, M.D., 2002. The WC1+ gd T-cell population in cattle: a possible role in resistance to intracellular infection. Vet. Immunol. Immunopathol. 89, 105–114.
Rusk, R.A., Palmer, M.V., Waters, W.R., Mcgill, J.L., 2017. Measuring bovine γδ T cell function at the site of Mycobacterium bovis infection. Vet. Immunol. Immunopathol. 193–194, 38–49.
Russell, D.G., 2006. Who puts the tubercle in tuberculosis? Nat. Rev. Microbiol. 5 (1), 39–47.
Stinson, K.J., Baquero, M.M., Plattner, B.L., 2018. Resilience to infection by Mycobacterium avium subspecies paratuberculosis following direct intestinal inoculation in calves. Vet. Res. 49 (1), 1–12.
Sweeney, R.W., 1996. Transmission of paratuberculosis. Vet. Clin. North Am. Food Anim. Pract. 12 (2), 305–312.
Telfer, J.C., Baldwin, C.L., 2015. Bovine gamma delta T cells and the function of gamma delta T cell specific WC1 co-receptors. Cell. Immunol. 296 (1), 76–86.
Verrall, A.J., Netea, M.G., Alisjahbana, B., Hill, P.C., van Crevel, R., 2013. Early clearance of *Mycobacterium tuberculosis*: a new frontier in prevention. Immunol. 141, 506–513.
Waters, W.R., Miller, J.M., Palmer, M.V., Stabel, J.R., Jones, D.E., Koistinen, K.A., Steadham, E.M., Hamilton, M.J., Davis, W.C., Bannantine, J.P., 2003. Early induction of humoral and cellular immune responses during experimental *Mycobacterium avium* subsp. *Paratuberculosis* infection of calves. Infect. Immun. 71 (9), 5130–5138.
Wyatt, C.R., Madruga, C., Cluff, C., Parish, S., Hamilton, M.J., Goff, W., Davis, W.C., 1994. Differential distribution of cd T-cell receptor lymphocyte subpopulations in blood and spleen of young and adult cattle. Vet. Immunol. Immunopathol. 40, 187–199.
Yasuda, M., Ogawa, D., Nasu, T., Yamaguchi, T., Murakami, T., 2005. Kinetics and distribution of bovine gd T-lymphocyte in the intestine: gd T cells accumulate in the dome region of Peyer's patch during prenatal development. Dev. Comp. Immunol. 29 (6), 555–564.